J Solid State Electrochem (2007) 11:482–489
DOI 10.1007/s10008-006-0184-1

ORIGINAL PAPER

Effect of aliovalent doping on the transport properties of lanthanum cuprates

A. Berenov · J. Wei · H. Wood · R. Rudkin · A. Atkinson

Received: 27 April 2006 / Revised: 24 May 2006 / Accepted: 30 May 2006 / Published online: 30 August 2006

Abstract Cuprates with perovskite-related structure and the general formula $La_{1-x}A_xCu_{1-y}B_yO_{2.5\pm\delta}$ (A=Ca, Ba, Sr; B=Li; x=0.1, 0.2, 0.3; y=0, 0.1) were prepared by the citrate route. Their structures were studied by X-ray powder diffraction and their electrical conductivities (as a function of temperature) by four-point DC measurements on sintered bars. The highest values of electrical conductivity were observed for the x=0.3 Sr-doped cuprate, which showed a metallike temperature dependence. Ba-doped cuprates showed a transition from semi-conducting to metallic temperature dependence of conductivity. The extent of A-site deficiency is small and had the effect of slightly decreasing the conductivity and thermal expansion coefficient. Li solubility was also found to be small, but it reduced conductivity drastically, due in part to the disruption of the copper–oxygen conductive network. Reactions between cuprates and a typical manganite fuel cell cathode, and Pt and Pd contacts were observed at 1,000 °C.

Keywords Lanthanum cuprate · Acceptor doping · Electrical conductivity · Solid oxide fuel cell

Introduction

In solid oxide fuel cells (SOFCs) the current must be collected from the electro-catalytic electrodes and carried out to the external circuit. Different SOFC designs employ different configurations and materials to achieve these current collection and cell inter-connection functions. Metals are a common choice of material for this, but they either suffer degradation by corrosion/oxidation, or are expensive. Oxides could avoid the corrosion problems (particularly on the cathode side), but their electronic conductivities are usually too low. However, there are some transition metal oxides that do exhibit high conductivities (>100 S cm^{-1}), particularly those based on Co or Cu. The Co-based perovskites (e.g. $La_{1-x}Sr_xCoO_3$) have very high conductivities, but unfortunately they also have much higher thermal expansion coefficients (e.g. >20 ppm K^{-1}) than other SOFC materials (10–12 ppm K^{-1}), which leads to thermo-mechanical stability problems.

Recently, copper-based high temperature superconductors were suggested as potential materials for cathodes ($YBa_2Cu_3O_{7-d}$ [1]) and secondary interconnects ($Ba_2Sr_2CaCu_2O_{8+d}$ [2]) in SOFCs. In addition, Yu et al. [3] studied Sr-doped cuprates as possible cathodes for SOFC. Thirty percent Sr substitution for La resulted in a considerable increase of the electrical conductivity reaching 2,400 and 830 S cm^{-1} at room temperature and 800 °C in air, respectively. No reaction between $La_{1-x}Sr_xCuO_{2.5}$ ($0.2<x<0.3$) and 8 mol% YSZ was detected at 800 °C, and low values of cathodic polarisation were observed at 750 and 800 °C [3]. However, the polarisation resistance was higher than for other common cathodes.

Low temperature properties of cuprates with the perovskite structure have been extensively studied since the discovery of superconductivity in related compounds [4–6]. The parent compound, $La_2Cu_2O_5$, is stable only in a narrow temperature range (999–1,012 °C) [7]. Sr substitution stabilises the orthorhombic ($0.15<x<0.2$) or tetragonal ($0.2<x<0.3$) perovskite structures [3], and $La_{1-x}Sr_xCuO_{2.5}$ can be prepared from individual oxides by solid-state

A. Berenov (✉) · J. Wei · H. Wood · R. Rudkin · A. Atkinson
Department of Materials, Imperial College London,
Exhibition Road,
London, SW7 2AZ, UK
e-mail: a.berenov@imperial.ac.uk

reaction at 1,000 [8] or 960 °C [3]. The structures of all cuprates with *A*/*B* ratio of 1 are related to the cubic perovskite by ordering of oxygen vacancies along the *c* direction. Different types of ordering result in different structures and copper coordination (octahedral, planar, pyramidal) [4]. Oxygen non-stoichiometry (with respect to the nominal value of 2.5 corresponding to copper in the divalent state) is mainly dependent on the extent of Sr doping [3]. A very weak dependence of the extent of oxygen non-stoichiometry on oxygen partial pressure (1–100 atm) was observed in the $La_{6.4}Sr_{1.6}Cu_{8-x}Fe_xO_{20}$ series of compounds [9]. Thus, acceptor doping on the *A* site results mainly in the oxidation of some divalent copper to trivalent copper, which can be regarded as electron hole charge carriers. Consequently, the electronic carrier density can be tailored by aliovalent doping on La and/or Cu sites and/or introduction of *A* site deficiency.

In our preliminary, study no formation of perovskite cuprate with (La+Ca)/Cu ratio of 1 was observed at 1,000 °C, which is in agreement with the La_2O_3–CaO–CuO phase diagram [10]. Consequently, in this article we report studies of the effects of Sr and Ba doping (on the *A* site) and Li doping (on the *B* site) on the stability, structure, thermal expansion and transport properties of cuprate ceramics with the perovskite-related structure. In addition, the effect of A-site deficiency was also investigated.

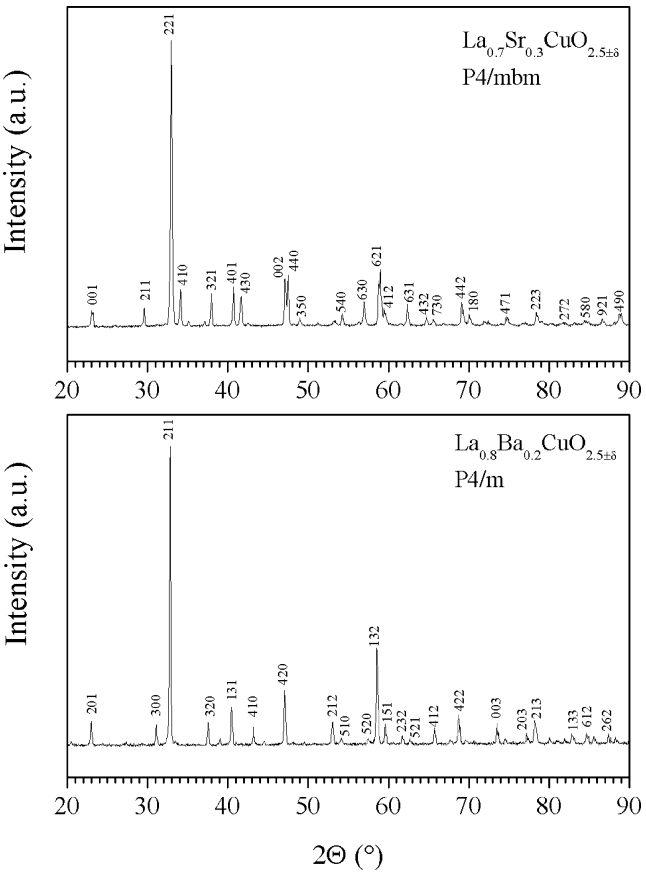

Fig. 1 XRD patterns of single phase Sr-doped (*top panel*) and Ba-doped (*bottom panel*) cuprates

Experimental

Acceptor-doped cuprates with the general formula $La_{1-x}A_xCu_{1-y}Li_yO_{2.5}$ (*A*=Sr, Ba; *B*=Li; *x*=0.1, 0.2, 0.3; *y*=0, 0.1) and A-site deficient cuprates with the general formula $La_{0.7-x}Sr_{0.3}CuO_{2.5}$ (*x*=0.025, 0.05) were prepared by the citrate route. Appropriate amounts of pre-calcined La_2O_3 (Alfa Aesar, 99.99%), ACO_3 (*A*=Sr, Ba; Alfa Aesar, 99.95%), Li_2CO_3 (Sigma Aldrich, 99.99%) and CuO (Alfa Aesar, 99.995%) were dissolved in nitric acid. Citric acid was added to the solution to give a citric ion to metal ion ratio of 1:1. The resulting gels were decomposed at 450 °C for 5 h. The residues were annealed in air at 900 °C for 10 h and then at 1,000 °C for 50 h with intermediate grinding to produce powders suitable for ceramic fabrication. Some of the powders were further annealed at 1,000 °C to improve the homogeneity of the products. For thermal expansion and electrical conductivity measurements, specimens (with approximate dimensions 3×2×25 mm) were isostatically pressed at 300 MPa and sintered at 1,000 °C for 2 h. The density of sintered specimens was measured by the Archimedes method.

Powder X-ray diffraction (XRD) patterns (Fig. 1) were recorded on a Philips 1710 diffractometer using monochromatic Cu Kα radiation. High temperature XRD data were collected on an X'Pert diffractometer by supporting the sample on a platinum strip in a Bühler HDK 2.2 furnace. The 'Unitcell' non-linear least square refinement program [11] was used to calculate the lattice parameters. The average oxidation state of Cu was determined by iodometric titration [3] with an error of less than ±0.01 units of valency. Electrical conductivity was measured by the four-point DC technique using Pt electrodes. Current in the range of 0.5–100 mA was supplied by a Keithley 224 current source, and voltages were measured using an Agilent 34401A digital multimeter. The direction of current was reversed during the measurements, and *I*–*V* curves were recorded at several temperatures. The thermal expansion coefficient was measured using a Netzsch-402E-dilatometer in static air with a heating rate of 10 °C/min.

To study chemical stability of the cuprates towards other materials, $La_{0.7}Sr_{0.3}CuO_{2.5}$ ceramic pellets were brushed with Pt (Ferro Corporation, USA) or Pd (Gwent Electronic Materials, UK) pastes and annealed in air at 900 °C for 183 and 163 h, respectively. In addition, a pellet was prepared by powder mixing 50 wt% $La_{0.7}Sr_{0.3}CuO_{2.5}$ and 50 wt% of the typical SOFC cathode material $(La_{0.8}Sr_{0.2})_{0.92}MnO_3$ (PraxAir, USA) and annealing in air at 1,000 °C for 10 h.

Results and discussion

Structure of doped cuprates

The crystal structure, phase composition and measured lattice parameters of the studied samples are given in Table 1.

Sr-doped cuprates The 10% Sr-doped cuprate specimen was not single phase. Torrance et al. [4] also reported that in $La_5SrCu_6O_{15}$ a small amount of $La_{2-x}Sr_xCuO_4$ phase was present according to magnetic susceptibility and XRD measurements. The major phase was an orthorhombic perovskite with the Pbam space group, which has lattice parameters related to the cubic perovskite (a_p) by $a \approx a_p 2\sqrt{2}$, $b \approx a_p\sqrt{2}$, $c \approx a_p$. Fu et al. [12] also reported the stabilisation of an orthorhombic phase with 14.29% Sr doping (produced at 1,020 °C in 1 bar oxygen) with similar crystal structure to the one observed here.

Twenty and 30% Sr-doped samples were found to be single-phase tetragonal crystal structure (P4/mbm), with parameters related to the cubic perovskite parent as $a \approx a_p 2\sqrt{2}$ and $c \approx a_p$. The a lattice parameter decreased with doping, whereas the c lattice parameter did not change significantly (Table 1). The average oxidation state of copper increased with the doping from 2.165±0.003 to 2.257±0.009 for 20 and 30% Sr-doped samples, respectively. The observed increase in the average oxidation state of copper can explain the reduction in the unit cell volume due to the formation of the smaller Cu^{3+} ion [13]. Similar levels of Sr doping in $La_{8-x}Sr_xCu_8O_{20-y}$ ($1.45<x<2.15$ corresponding to 18 to 27% Sr doping) were observed by Tamegai and Iye [6] to have similar effects on the lattice parameter to those found here.

Ba-doped cuprates Within the studied doping range, only the 20% A site-doped sample was a single-phase compound. It crystallises in a tetragonal structure (space group P4/m), which is related to the cubic perovskite parent cell as $a \approx a_p\sqrt{5}$ and $c \approx a_p$. Vijayaraghan et al. [5] prepared single-phase compounds with composition ranging from $La_4BaCu_5O_{13}$ (20% doping) to $La_3Ba_2Cu_5O_{13}$ (40% doping) by solid state reaction in air at 1,000 °C, followed by oxygenation at 527 °C. Lattice parameters for the 20%-doped cuprate in the present study compare well with the literature data [5, 14]. The average copper oxidation state was measured by iodometry to be 2.359±0.001 corresponding to the formula $La_4BaCu_5O_{12.9}$. The measured oxygen content is slightly smaller than values of 12.9 [19], 13.2 [14] and 13.4 [15] reported by others from thermo-gravimetric measurements.

Li-doped cuprates Li doping at the levels studied here resulted in the formation of multiphase specimens (except for the nominal composition $La_{0.8}Sr_{0.2}Cu_{0.9}Li_{0.1}O_{2.5-y}$) with the main perovskite phases retaining the structure of the parent (Li-free) compounds. This indicates that the equilibrium solubility level of Li is probably less than 10% of the Cu content. The a lattice parameter increased with Li substitution, whereas c remained unchanged. The measured average oxidation state of Cu in the sample with nominal composition $La_{0.8}Ba_{0.2}Cu_{0.9}Li_{0.1}O_{2.5-y}$ slightly decreased from 2.359±0.001 to 2.347±0.006. Consequently, the negative charge of the Li'_{Cu} defects is probably compensated by the formation of oxygen vacancies. The formation of oxygen vacancies and incorporation of the slightly larger Li^+ (ionic radii of Li^+ [6] and Cu^{2+} [6] are 0.76 and 0.73 Å [13], respectively) ions explains the increase of unit cell volume. Zenitani et al. [16] reported CuO as an impurity

Table 1 Crystallographic data and chemical composition of $La_{1-x}A_xCu_{1-y}Li_yO_{2.5}$ compounds

Compound	Crystal structure/space group	Lattice parameters (Å)	Impurity phases	Average oxidation state of copper
$La_{0.9}Sr_{0.1}CuO_{2.5}$	Orthorhombic, Pbam	a=5.527(5), b=10.512(6), c=3.868(2)	$(La,Sr)_2CuO_4$, CuO	NA
$La_{0.8}Sr_{0.2}CuO_{2.5}$	Tetragonal, P4/mbm	a=10.840(3), c=3.859(2)	Not present	2.165±0.003
$La_{0.7}Sr_{0.3}CuO_{2.5}$	Tetragonal, P4/mbm	a=10.823(2), c=3.855(1)	Not present	2.257±0.009
$La_{0.8}Sr_{0.2}Cu_{0.9}Li_{0.1}O_{2.5}$	Tetragonal, P4/mbm	a=10.835(5), c=3.862(2)	$(La,Sr)_2CuO_4$, $La_2SrCu_2O_6$	NA
$La_{0.7}Sr_{0.3}Cu_{0.9}Li_{0.1}O_{2.5}$	Tetragonal, P4/mbm	a=10.833(2), c=3.855(1)	$(La,Sr)_2CuO_4$, $La_2SrCu_2O_6$	NA
$La_{0.675}Sr_{0.3}CuO_{2.5}$	Tetragonal, P4/mbm	a=10.8301(3), c=3.858(2)	$(La,Sr)_2CuO_4$	2.246±0.002
$La_{0.65}Sr_{0.3}CuO_{2.5}$	Tetragonal, P4/mbm	a=10.837(4), c=3.859(3)	$(La,Sr)_2CuO_4$	2.238±0.009
$La_{0.9}Ba_{0.1}CuO_{2.5}$	Tetragonal, P4/m	a=8.640(2), c=3.865(4)	$(La,Ba)_2CuO_4$	NA
$La_{0.8}Ba_{0.2}CuO_{2.5}$	Tetragonal, P4/m	a=8.643(3), c=3.865(1)	Not present	2.359±0.001
$La_{0.7}Ba_{0.3}CuO_{2.5}$	Tetragonal, P4/m	a=8.650(5), c=3.864(2)	$(La,Ba)_2CuO_4$	NA
$La_{0.8}Ba_{0.2}Cu_{0.9}Li_{0.1}O_{2.5}$	Tetragonal, P4/m	a=8.661(5), c=3.865(7)	$(La,Ba)_2CuO_4$	2.347±0.006

phase in their Li-doped specimens of nominal composition $La_8Cu_{8-x}Li_xO_{20}$ (x=0.4–1.2) and also observed an increase in the lattice parameters of the majority phase.

Electrical conductivity of doped cuprates

The relative density of specimens used for electrical measurements was typically 80–98%. At the intermediate levels of the relative density (50–90%), the values of electrical conductivity depends on the relative density, d, as $\sigma \sim d^{\beta}$, where the value of parameter β is sample-specific [17]. When the relative density is higher, then 90% the relationship between the electrical conductivity and the relative density is linear [18]. In this study, no correction was applied to take account of the porosity in the specimens.

Sr-doped cuprates Sr-doped cuprates showed a decrease in conductivity with increasing temperature, which is a characteristic feature of metallic conductivity (Fig. 2). However, this does not necessarily imply true metallic conduction, as characterised by a concentration of carriers that is independent of temperature and a carrier mobility that decreases with temperature due to phonon scattering. The observed temperature dependence could, for example, be due to a decrease in carrier concentration with temperature as more oxygen vacancies are created. The following defect-forming reactions are possible (using Kröger–Vink notation):

$$null \rightarrow e' + h^{\bullet} \tag{1}$$

$$null \rightarrow 2e' + v_O^{\bullet\bullet} + \frac{1}{2}O_2 \tag{2}$$

On a localised charge (small polaron) model, the electron hole can be regarded as a Cu^{3+} ion. The electrical neutrality condition is

$$\left[Sr'_{La}\right] + n = 2\left[v_O^{\bullet\bullet}\right] + p \tag{3}$$

An increase in the extent of Sr doping was observed to enhance the electrical conductivity, presumably due to an increase in the hole carrier concentration as determined by chemical analysis. $La_{0.7}Sr_{0.3}CuO_{2.5}$ showed the highest values of electrical conductivity ranging from 3,260 S cm^{-1} at room temperature to 500 S cm^{-1} at 1,000 °C (Fig. 2). The observed values of the electrical conductivity and the metallic-type temperature dependence are in qualitative agreement with other reports in the literature [3, 8]. After the electrical measurements at 1,000 °C, the formation of Sr_3CuPtO_6 and $(La,Sr)_2CuO_4$ impurities was observed by XRD in $La_{0.7}Sr_{0.3}CuO_{2.5}$ specimen suggesting poor chemical stability of the cuprates.

Ba-doped cuprates At room temperature, the conductivity of $La_{0.8}Ba_{0.2}CuO_{2.5}$ was 326 S cm^{-1}, which is within the wide range of values quoted for the Ba-doped cuprate: 285 [6] to 1.6×10^4 S cm^{-1} [15]. The temperature dependence of conductivity is shown in Fig. 3. Hysteresis effects in the electrical conductivity were observed during heating and cooling due to the sluggish equilibration kinetics. In run 1 (Fig. 3) at the intermediate temperatures (200–700 °C), long dwell times of up to 24 h were required to obtain constant, stable values of electrical conductivity both upon heating and cooling. In run 2 (Fig. 3) with the same specimen, measurements were taken on heating and then on cooling with a constant temperature ramp rate of 0.5 °C/min. Hysteresis is evident at temperatures below approximately 700 °C, but at higher temperatures reproducible values of conductivity were observed regardless of heating

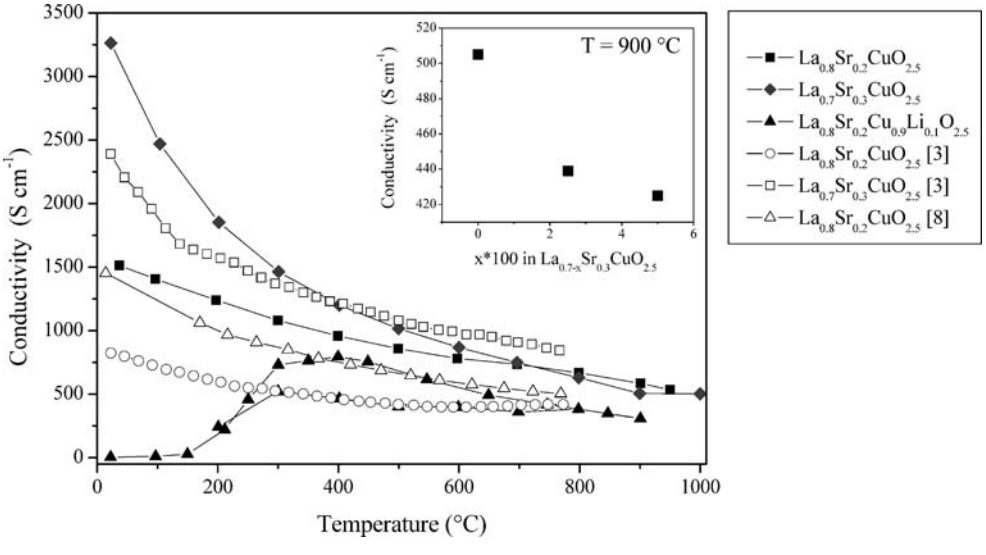

Fig. 2 The electrical conductivity of Sr-doped cuprates as a function of temperature. The *solid lines* only serve as guides and are not relevant

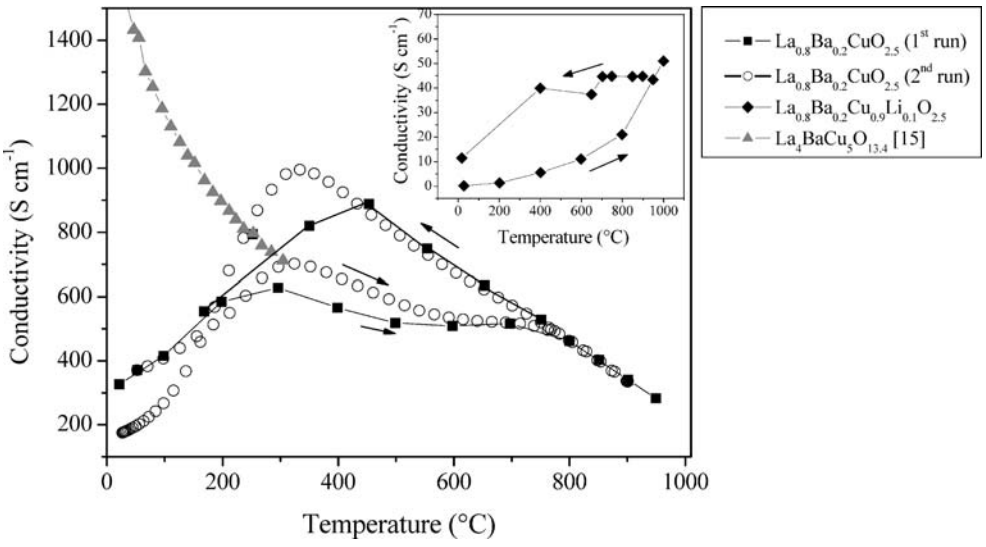

Fig. 3 The electrical conductivity of Ba-doped cuprates as a function of temperature. The *solid lines* only serve as guides and are not relevant

or cooling or thermal history. The formation of small amounts of CuO and $(La,Ba)_2CuO_4$ were observed by XRD after the electrical measurements. A transition from semi-conducting to metallic-like behaviour was observed at around 320 °C. The observation of semi-conducting behaviour at the lower temperatures contradicts the results of some previous studies in which metallic behaviour was observed in $La_4BaCu_5O_{13.4}$ in air over a wide temperature range (20–300 K [5], 5–270 K [4, 6] and 200–600 K [15]). However, a change from metallic-type to semi-conducting behaviour was observed by Vijayaraghavan et al. [5] when $La_4BaCu_5O_{13.4}$ was heated in nitrogen or a H_2/N_2 mixture. They suggested that this change was due to an increase in oxygen vacancies and corresponding decrease in the oxygen content to a value below $La_4BaCu_5O_{13}$. In the present study, no significant change in the average oxidation state of copper before (2.359±0.001) and after (2.366±0.003) the electrical measurements was observed by chemical analysis suggesting that our specimens maintain an oxygen content at low temperatures corresponding to $La_4BaCu_5O_{12.9}$. Michael et al. [15] did not observe any change of oxygen content by thermo-gravimetric analysis of this composition up to 850 °C. On the contrary, Anderson et al. [19] reported detectable oxygen loss at temperatures above 770 °C. They found that the changes of oxygen stoichiometry were reversible upon cooling. However, no value of heating and cooling rates was given. The temperature above which they observed reversible changes in the oxygen stoichiometry (770 °C) is very close to the one above which reproducible values of conductivity were measured in this work. This suggests that the metallic-like behaviour observed in this temperature range is due to a reduction in the hole carrier concentration (and increase in oxygen vacancy concentration) and not a mobility with negative temperature dependence.

Alternatively, the apparent metal to semi-conductor transition may be related to structural changes similar to the orthorhombic to tetragonal transition in $YBa_2Cu_3O_y$ at 350 °C [20]. In situ high temperature XRD was therefore carried out in air up to 800 °C. $La_4BaCu_5O_{12.9}$ maintained the tetragonal crystal structure during both heating and cooling. No change in peak position was detected between scans collected after 30 min and 5 h anneal at the intermediate temperature range (200–500 °C) suggesting that the long equilibrium time observed during the resistivity measurements is not linked to significant structural changes. Good reproducibility of the unit cell parameters during heating and cooling was observed (Fig. 4). The *a* lattice parameter showed linear thermal expansion corresponding to a thermal expansion coefficient (TEC) of 18.5×10^{-6} K^{-1}. This value of TEC is close to the values determined by dilatometry of Sr-doped cuprates [23]. Consequently, the observed apparent metal to semi-

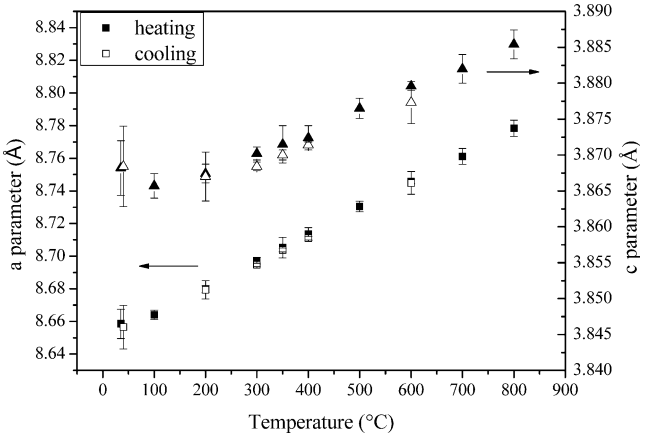

Fig. 4 Variation of lattice parameters of $La_{0.8}Ba_{0.2}CuO_{2.5}$ with temperature in air

conductor transition is unlikely to be caused by the changes in crystal structure.

Li-doped cuprates Li-doped samples, namely, $La_{0.8}Ba_{0.2}Cu_{0.9}Li_{0.1}O_{2.5}$ (Fig. 3) and $La_{0.7}Sr_{0.3}Cu_{0.9}Li_{0.1}O_{2.5}$ (not shown), exhibited semi-conducting behaviour with values of conductivity significantly decreased in comparison with the Li-free analogues. This decrease in electrical conductivity contradicts the results of Zenitani et. al. [16], who observed an increase in the conductivity with Li doping in $La_8Cu_{8-x}Li_xO_{20}$ ($0.4<x<1.2$). However, their specimens had no other acceptor dopants (Sr and Ba in the present study) and were prepared at higher oxygen partial pressure than our specimens. In addition, the exact stoichiometry of their samples is unclear as the mixtures of $La_8Cu_8O_{20}$, CuO and Li_2CO_3 that were used during the synthesis may have resulted in the formation of *A*-site deficient material. The electrical conductivity of $La_2Cu_{1-x}Li_xO_4$ cuprates with the K_2NiF_4 structure showed a complex dependence on Li doping level [21]. The room temperature conductivity increased at small doping levels (up to 10%) reaching a broad maximum and showed a sharp decrease when the Li concentration exceeded 30%. The observed effect was explained by the competition between increased carrier (hole) concentration and the disorder introduced into the conductive CuO_2 planes. The decrease in the conductivity observed in the present study is suggested to be caused by a combination of the following: a decrease in the carrier concentration (as determined by an average copper oxidation state discussed above), disorder of the Cu conducting network by Li^+ ions, and/or the presence of lower conductivity impurity phases. The reduction in conductivity observed after the substitution of foreign ions into the copper site could be attributed to carrier trapping [8]. However, the effect of carrier trapping on electrical conductivity has not been studied in detail. For example, Genouel et al. [9] synthesised a series of doubly substituted perovskites, $La_{6.4-x}Sr_{1.6+x}Cu_{8-x}Fe_xO_{20}$ ($0<x<2$), in which the oxidation state of copper was designed to remain almost constant. They observed that the room temperature conductivity decreased by one order of magnitude when 20% of the Cu was substituted by Fe ($x=0.2$).

A-site deficiency in cuprates

A-site deficient cuprates $La_{0.7-y}Sr_{0.3}CuO_{2.5}$ ($y=0.025$, 0.05) crystallised in the tetragonal perovskite structure (P4/mbm). Both *a*- and *c*-lattice parameters increased with the extent of the *A*-site deficiency. XRD showed the presence of $(La,Sr)_2CuO_4$ impurity phase in the *A*-site deficient samples. Further anneals at 1,000 °C for 50 h did not result in the formation of homogeneous specimens. The presence of the impurity phase with the *A*/*B* ratio of 2 and the absence of CuO in the nominally La-deficient ceramics suggests that the extent of the La-deficient region is greater than 2.5%. Chemical analysis showed that the average oxidation state of copper decreased slightly with the *A*-site deficiency from 2.257±0.009 in the stoichiometric compound to 2.246±0.002 and 2.238±0.009 in $La_{0.675}Sr_{0.3}CuO_{2.5}$ and $La_{0.65}Sr_{0.3}CuO_{2.5}$*A*-site deficient compounds, respectively. Therefore, the dominant compensation mechanism of negatively charged *A*-site vacancies is believed to be the formation of oxygen vacancies and not holes. Since Sr substitution for La favours holes rather than oxygen vacancies, this implies an attractive association of the *A*-site vacancies and oxygen vacancies that lowers the effective formation energy of the oxygen vacancies.

A-site deficient samples showed metallic temperature dependence similar to that of the stoichiometric parent compound, $La_{0.7}Sr_{0.3}CuO_{2.5}$. The effect of the nominal *A*-site deficiency on the conductivity values at 900 °C is shown in the inset of Fig. 2. The conductivity decreased with the increase of the extent of the *A*-site deficiency presumably due to the decrease in the charge carrier concentration and/or the presence of the more resistive $(La,Sr)_2CuO_4$ impurity phase [22]. Nevertheless, conductivity values at 900 °C as high as 425 S cm^{-1} were observed in the cuprate with 5% nominal *A*-site deficiency. No other impurity phase than $(La,Sr)_2CuO_4$ was observed after the electrical measurements.

Thermal expansion curves, measured by dilatometry, for the *A*-site deficient cuprates are shown in Fig. 5. Good linearity of the data was observed within the 50–900 °C temperature range. The average thermal expansion coefficient (TEC) values decreased from 15.1×10^{-6} K^{-1} for $La_{0.675}Sr_{0.3}CuO_{2.5}$ to 14.2×10^{-6} K^{-1} for $La_{0.65}Sr_{0.3}CuO_{2.5}$. These TEC values are smaller than those for stoichiometric cuprates (around 17×10^{-6} K^{-1} [23]) and closer to that of the YSZ SOFC electrolyte. The presence of porosity in the specimens is not expected to affect the values of the thermal expansion coefficient [24]. Consequently, the introduction of nominal *A*-site deficiency into Sr-doped cuprates decreases the thermal expansion mismatch between cuprate and YSZ at the expense of only slight degradation of electrical performance.

Stability towards SOFC components

Chemical compatibility of the Sr-doped cuprates was evaluated with respect to materials that they might be in contact with during testing or operation (Pd, Pt and LSM). Annealing $La_{0.7}Sr_{0.3}CuO_{2.5}$ pellets with Pt and Pd paste contacts at 700 °C for up to 60 h did not show any signs of

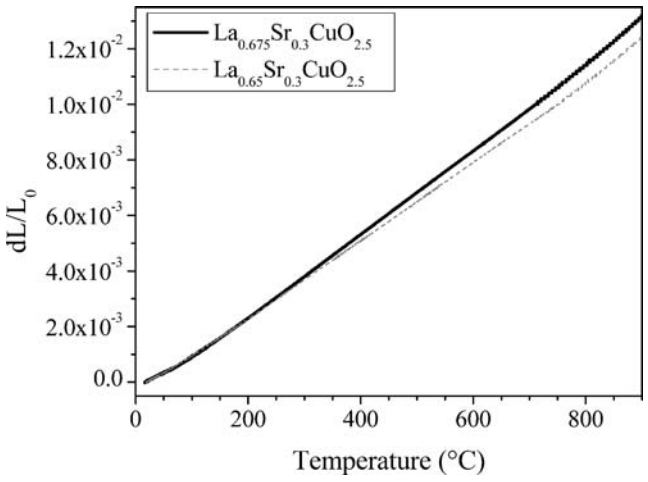

Fig. 5 Dilatometric curves of A-site deficient cuprates as a function of temperature

chemical reactions. However, prolonged anneals at 900 °C resulted in the reaction of Pd and Pt with the cuprate to form new phases detectable by XRD (Fig. 6). In the case of Pt, the interaction product peaks were assigned to $La_{2-x}Sr_xCuO_4$, Sr_4PtO_6 and CuO. Chemical reaction of the Cu-containing phase $Bi_2Sr_2CuO_6$ with Pt crucibles at 1,100 °C was reported [25]. In the case of Pd, the interaction product XRD peaks were assigned to $La_2Pd_2O_5$, $SrPd_3O_4$ and Sr_2PdO_3. Substitution of Pd in La_2CuO_4 at 700 °C was also reported [26].

Annealing of $La_{0.7}Sr_{0.3}CuO_{2.5}$ and $(La_{0.8}Sr_{0.2})_{0.92}MnO_3$ powder mixture at 1,000 °C for 10 h resulted in the formation of a single-phase orthorhombic perovskite. Interdiffusion of constituents in perovskite-related structures is to be expected, and similar examples were reported. Single-phase $LaMn_{1-x}Cu_xO_{3-y}$ perovskites, with x up to 0.6, were prepared by freeze-drying of nitrates followed by annealing at 1,100 °C [27]. The chemical stability of $YBa_2Cu_3O_7$ (YBCO) towards some SOFC materials has been studied by Arul Raj et al. [28]. They observed reaction products (La_2CuO_4 and $CuCO_3$) on annealing a mixture of YBCO and $La_{0.65}Sr_{0.3}MnO_3$ at 800 °C for 2 weeks. In addition, corrosion layers were formed between YBCO and a ferritic steel after a long anneal at 800 °C. Therefore, high reactivity of Cu-containing perovskites towards other SOFC materials is likely to limit their useable temperatures to below 700 °C.

Conclusions

Single-phase cuprates with aliovalent doping on the *A* site ($La_{0.8}Sr_{0.2}CuO_{2.5-y}$, $La_{0.7}Sr_{0.3}CuO_{2.5-y}$, $La_{0.8}Ba_{0.2}CuO_{2.5-y}$) were prepared by the citrate route. The highest values of conductivity were observed for the 30% Sr-doped cuprate and also exhibited metallike temperature dependence. The 20% Ba-doped cuprate showed an apparent transition from semi-conducting behaviour at temperatures below approximately 300 °C to metallic behaviour at higher temperatures. This perovskite also exhibited hysteresis in electrical conductivity below 700 °C, which is consistent with sluggish kinetics of oxygen uptake or loss at temperatures below 700 °C.

Attempts to dope Li on the *B* site showed that the Li solubility was small (probably <10%). $La_{0.8}Ba_{0.2}Cu_{0.9}Li_{0.1}O_{2.5-y}$ appeared as single phase by XRD, but the Li doping on the Cu site resulted in much lower conductivity.

Introduction of *A*-site deficiency in $La_{0.7-y}Sr_{0.3}CuO_{2.5}$ (y=0.025, 0.05) slightly decreased electrical conductivity, but also decreased the thermal expansion coefficient significantly.

At 900 °C cuprates were observed to form reaction products when in contact with Pt or Pd and formed a

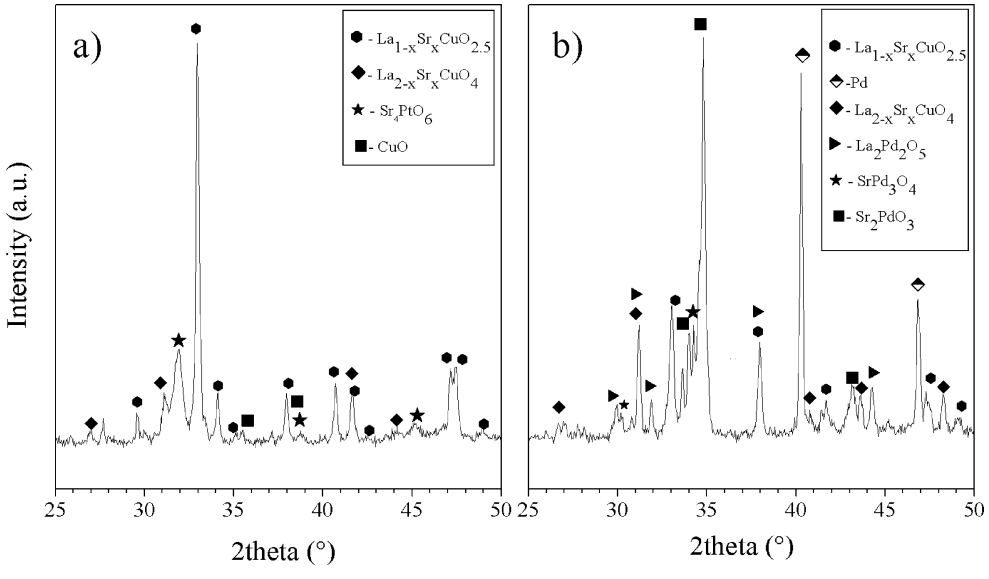

Fig. 6 XRD patterns of $La_{0.7}Sr_{0.3}CuO_{2.5}$ pellets with Pt (**a**) and Pd (**b**) coatings after annealing at 900 °C for 183 and 163 h, respectively

mixed, single-phase perovskite by inter-diffusion with $(La_{0.8}Sr_{0.2})_{0.92}MnO_3$.

Acknowledgments Financial support from Rolls-Royce Fuel Cell Systems Ltd and the European Commission (Project PIP-SOFC) are duly acknowledged. The authors also thank Mr. R. Sweeney for the assistance with high temperature XRD measurements.

References

1. Chang C-L, Lee T-C, Huang T-J (1998) J Solid State Electrochem 2:291
2. Tietz F, Arul Raj I, Jungen W, Stover D (2001) Acta Mater 49:803
3. Yu HC, Fung KZ (2003) Mater Res Bull 38:231
4. Torrance JB, Tokura Y, Nazzal A, Parkin SSP (1988) Phys Rev Lett 60:542
5. Vijayaraghavan R, Ram RAM, Ganguly P, Rao CNR (1988) Mater Res Bull 23:719
6. Tamegai T, Iye Y (1989) Physica C 159:181
7. Hiroi Z (1996) J Solid State Chem 123:223
8. Skinner SJ, Munnings C (2002) Mater Lett 57:594
9. Genouel R, Michel C, Nguyen N, Hervieu M, Raveau B (1995) J Solid State Chem 115:469
10. Skakle JMS, West AR (1994) J Am Ceram Soc 77:2199
11. Holland TJB, Redford SAT (1997) Mineral Mag 61:65
12. Fu WT, Drost RJ, Ijdo DJW, Frikkee E (1994) Mater Res Bull 29:629
13. Shannon RD (1976) Acta Crystallogr A32:751
14. Shivakumara C, Hegde MS, Sooryanarayana K, Guru Row TN, Subbanna GN (1998) J Mater Chem 8:2695
15. Michel C, Er-Rakho L, Raveau B (1985) Mater Res Bull 20:667
16. Zenitani Y, Watanabe N, Akimitsu J (2000) Physica C 341–348:355
17. Roosmalen JAM, Huijsmans JPP, Cordfunke EPH (1991) In: Gross F, Zegers P, Singhal SC, Yamamoto O (eds) Proceedings of the 2nd International Symposium on SOFC, Athens, Greece, 2–5 July 1991, p 507
18. Kertesz M, Riess I, Tannhauser DS (1982) J Solid State Chem 42:125
19. Anderson PS, Kirk CA, Skakle JMS, West AR (2003) J Solid State Chem 170:1
20. Freitas PP, Plaskett TS (1987) Phys Rev B 36:5723
21. Sarrao JL (1996) Phys Rev B 54:12014
22. Opila EJ, Pfundtner G, Maier J, Tuller HL, Wuensch BJ (1992) Mater Sci Eng B 13:165
23. Yu HC, Fung KZ (2004) J Power Sources 133:162
24. Boccaccini AR (1997) Eur Phys J Appl Phys 2:197
25. Hodeau JL (1992) Acta Crystallogr B 48:1
26. Guilhaume N, Peter SD, Primet M (1996) Appl Catal B 10:325
27. Gallagher PK, Johnson DW, Vogel EM (1977) J Am Ceram Soc 60:28
28. Arul Raj I, Tietz F, Gupta A, Jungen W, Stover D (2001) Acta Mater 49:1987